Fluid Phase Equilibria 530 (2021) 112885

Contents lists available at ScienceDirect

Fluid Phase Equilibria

journal homepage: www.elsevier.com/locate/fluid

Assessment of scaled particle theory predictions of the convergence of solvation entropies

Henry S. Ashbaugh

Department of Chemical and Biomolecular Engineering, Tulane University, New Orleans, LA 70118, USA

ARTICLE INFO

Article history:
Received 27 August 2020
Revised 9 October 2020
Accepted 25 October 2020
Available online 4 November 2020

Keywords:
Hydrophobic effects
Statistical thermodynamics
Hydration
Scaled particle theory

ABSTRACT

Entropy convergence is the experimental observation that the hydration entropies of families of non-polar solutes cross one another and converge at a distinct temperature above the boiling point of water. Entropy convergence has subsequently received significant theoretical and molecular simulation interest to interpret its molecular origin. Classic scaled particle theory has enjoyed success in describing entropy convergence for cavity-like, hard sphere solutes in water despite the fact it only considers water's equation-of-state and effective hard sphere diameter while neglecting liquid state inter-molecular correlations. This stands in difference to traditional interpretations of the hydrophobic effect that invoke water's three-dimensional structure when describing aqueous solutions of non-polar moieties. Here we investigate the origins of entropy convergence in classic scaled particle theory. We demonstrate convergence results from the theory's unphysical prediction that the surface tension of the solvent against a hard, flat interface exhibits a maximum as a function of temperature, indicative of a surface entropy that changes sign from negative to positive values with increasing temperature. In addition, we find that classic scaled particle theory can predict convergence like behavior in an organic liquid for which the phenomenon is unexpected.

The poor solubility of non-polar solutes in water at room temperature is characterized by a favorable negative hydration enthalpy that is opposed by an even more unfavorable negative hydration entropy. The enthalpy and entropy both depend markedly on temperature as indicated by a large positive heat capacity increment. These thermodynamic quantities give rise to a nearly parabolic dependence of the hydration free energy on temperature with a maximum at the point the entropy crosses zero. Taken together these properties are considered thermodynamic finger prints of the hydrophobic effect [1–4]. These stand in contrast to solvation in most other liquids, where solvation is usually opposed by the enthalpy, and the solvation properties are not as significantly temperature dependent. Beyond these characteristics, hydrophobic hydration is accompanied by additional thermodynamic puzzles that pose challenges to the development of a unified molecular understanding of hydrophobic effects [5].

The observation of entropy convergence for non-polar solute hydration has attracted scientific scrutiny since the 1980s. Entropy convergence is the phenomenon that when the entropies of hydrophobic solutes are plotted as a function of temperature, they appear to converge to one another at distinct temperatures. The observed convergence temperatures can depend on the class of solutes considered, *e.g.*, noble gases versus alkanes or aromatics, but generally speaking range from approximately 100°C to 130°C [6–12]. It is notable that the inference of convergence relies on extrapolation of solubility data beyond the normal boiling point of water, let alone beyond the temperature range reliable results are available. The convergence temperature typically falls below the maximum in the hydration free energy, indicating the convergence entropy is negative. Nevertheless, the convergence temperature frequently only narrowly proceeds the free energy extremum. The apparent correspondence between the entropy convergence temperature of the hydrocarbons and the thermodynamics of unfolding of proteins prompted Baldwin [11,13] to hypothesize that protein folding could be interpreted in the context of Kauzmann's hydrocarbon core model [14]. Expansion of the available protein folding thermodynamic datasets, however, called this idea into doubt [15]. Nevertheless, entropy convergence for smaller solutes persists as an enduring observation.

Molecular simulations of model solutes and statistical thermodynamic theories have been used to try to gain fundamental insight into the origin of entropy convergence phenomena in water. To simplify the description of solute/water interactions, the solute in these studies is frequently assumed to act as a hard sphere cav-

E-mail address: hanka@tulane.edu

https://doi.org/10.1016/j.fluid.2020.112885
0378-3812/

ity that excludes water oxygens. The rationale for this approximation is that solvation free energies in general can be divided between contributions from forming a cavity the size and shape of the solute and the work associated with turning on attractive interactions between the solute and solvent. The free energy of forming a solute sized cavity is known to dominate the thermodynamics of hydrophobic hydration, while solute/solvent attractions can be treated perturbatively. As a result, cavity-like solutes are thought to be ideal for isolating the essential elements of hydrophobic hydration. Garde *et al.* [16] demonstrated entropy convergence for simple gases in simulations of water. Their analysis based on information theory linked convergence to Gaussian fluctuations in water's local density that are effectively temperature independent as a result of water's isothermal compressibility being relatively insensitive to temperature. Netz and co-workers [17], on the other hand, found from simulations that the convergence temperature sensitively depends on the softness of small solute cavities, with harder cavities exhibiting higher convergence temperatures. They inferred that convergence only occurs between solutes within a homologous series that differ only in the number of sites comprising the solute. A follow up study of spherical and cylindrical solutes found that the entropy convergence temperature sensitively depends on the solute curvature and disappears with increasing solute size, although some details may be attributable to the model used to simulate water [18]. Huang and Chandler [19] examined the hydration of cavity-like solutes over a wide range of solute radii using Lum, Chandler, and Weeks theory [20]. They found for solutes with hard sphere radii 14 Å and larger, the potential for entropy convergence is non-existent due to the macroscopic surface tension dominating the free energy which makes a positive contribution to the entropy.

Scaled particle theory (SPT) provides an alternate approach to deriving the solubilities of cavity-like solutes. SPT takes the view that the excess chemical potential associated with solvating a hard, spherical cavity can be evaluated from the work of inflating that cavity from nothing to a cavity with a solvent excluding radius R. SPT was originally developed to model hard sphere fluids [21] although it was recognized that this analytical framework could be extended to realistic solvents by utilizing their experimental densities and pressures [22,23]. We refer to this as classic SPT (CSPT). CSPT has been used since the 1960s to interpret the meager solubilities of non-polar species in water going back to the influential work of Pierotti [24–26]. A number of CSPT studies have investigated the origin of entropy convergence phenomena, obtaining results that agree reasonably well with experimental convergence temperatures [12,27,28]. While CSPT utilizes experimental equation-of-state information about the solvent, it does not contain molecular-scale information beyond the effective hard sphere diameter of the solvent. Recognizing solvent structure plays a critical role in understanding the hydrophobic effect, Stillinger expanded SPT to incorporate pair-wise water correlations determined from scattering experiments within its framework [29]. We subsequently extended Stillinger's work to utilize multi-body solvent correlations obtained from molecular simulation to improve the description of cavity solvation from microscopic to macroscopic solutes [10,30,31]. We refer to this approach as revised SPT (RSPT). Much like Netz and Chandler's work, RSPT calls into question the occurrence of a distinct convergence temperature. Nevertheless, questions remain as to why CSPT captures entropy convergence in aqueous solutions. Here, we probe CSPT's description of entropy convergence in an effort to understand the theoretical rationale for its success.

In CSPT, the solute cavity size R denotes the solvent excluding radius as determined by the sum of the van der Waals radii of the solvent (s) and cavity (c), *i.e.*, $R = (\sigma_{ss} + \sigma_{cc})/2$ where σ_{ss} and σ_{cc} are the solvent and cavity diameters. The excess chemical potential of the cavity solute is evaluated in CSPT as a cubic polynomial of the cavity radius

$$\mu_c^{ex} = k_BT\left\{\left[-\ln(1-\eta) + \frac{9\eta^2}{2(1-\eta)^2} - \frac{\eta P}{RT\rho}\right] + \left[-\frac{3\eta(1+2\eta)}{(1-\eta)^2} + \frac{3\eta P}{RT\rho}\right]\left(\frac{2R}{\sigma_{ss}}\right) + \left[\frac{3\eta(2+\eta)}{2(1-\eta)^2} - \frac{3\eta P}{RT\rho}\right]\left(\frac{2R}{\sigma_{ss}}\right)^2 + \frac{\eta P}{RT\rho}\left(\frac{2R}{\sigma_{ss}}\right)^3\right\}, \quad (1)$$

where k_BT is the product of Boltzmann's constant and the absolute temperature, P is the bulk pressure, ρ is the bulk solvent number density, and $\eta = \pi\sigma_{ss}^3\rho/6$ is the solvent packing fraction. The chemical potential in this expression denotes the solvation free energy of the solute in excess of the ideal gas contribution as determined in Ben-Naim's standard state [32]. This expression applies for solutes with $R \geq \sigma_{ss}/2$, which implies $\sigma_{cc} \geq 0$. Smaller radii correspond to cavities with negative van der Waals diameters, which are important in the development of SPT but are not physically meaningful when describing realistic solutes. While R may be the most natural size metric for expanding the chemical potential since the solvent force against which the solute is inflated is exerted only at the solvent excluded surface for a hard cavity, this expression may be simplified using alternate size measures. Recasting Eq. (1) by substituting $2R/\sigma_{ss} = \sigma_{cc}/\sigma_{ss} + 1$ for the size dependence, this expression can be equivalently expressed as a cubic polynomial of the cavity's van der Waals diameter

$$\mu_c^{ex} = k_BT\left[-\ln(1-\eta) + \frac{3\eta}{(1-\eta)}\left(\frac{\sigma_{cc}}{\sigma_{ss}}\right) + \frac{3\eta(2+\eta)}{2(1-\eta)^2}\left(\frac{\sigma_{cc}}{\sigma_{ss}}\right)^2\right] + \frac{\pi P}{6}\sigma_{cc}^3. \quad (2)$$

Here we evaluate the solute excess chemical potential and entropy using this formula since σ_{ss} can depend on the temperature and pressure itself for realistic solvents, thereby complicating evaluation of thermodynamic derivatives of R. The excess solvation entropy of the cavity solute can be evaluated by taking the temperature derivative of Eq. (2) at constant pressure and cavity van der Waals diameter

$$s_c^{ex} = -\left.\frac{\partial\mu_c^{ex}}{\partial T}\right|_{P,\sigma_{cc}} = k_B\left\{\left[\frac{\eta}{(1-\eta)}T\tilde{\alpha} + \ln(1-\eta)\right] + \left[\frac{3\eta}{(1-\eta)^2}T\tilde{\alpha} + \frac{3\eta}{(1-\eta)}\left(T\left.\frac{\partial ln\sigma_{ss}}{\partial T}\right|_P - 1\right)\right]\left(\frac{\sigma_{cc}}{\sigma_{ss}}\right) + \left[\frac{3\eta(1+2\eta)}{(1-\eta)^3}T\tilde{\alpha} + \frac{3\eta(2+\eta)}{2(1-\eta)^2}\left(2T\left.\frac{\partial ln\sigma_{ss}}{\partial T}\right|_P - 1\right)\right]\left(\frac{\sigma_{cc}}{\sigma_{ss}}\right)^2\right\}. \quad (3)$$

While σ_{cc} is temperature independent in this expression, we have allowed σ_{ss} to depend on temperature, necessitating inclusion of the derivative $\partial ln\sigma_{ss}/\partial T|_P$. The term $\tilde{\alpha}$ is the packing fraction expansivity ($\tilde{\alpha} = -\partial ln\eta/\partial T|_P = -\partial ln\rho/\partial T|_P - 3\partial ln\sigma_{ss}/\partial T|_P$), which reduces to the thermal expansion coefficient of the solvent when σ_{ss} is constant ($\partial ln\sigma_{ss}/\partial T|_P = 0$). Eqs. (2) and (3) form the basis for our analysis of entropy convergence as predicted by CSPT.

While σ_{ss} is frequently assumed to be fixed, some implementations of CSPT invoke a thermodynamic state dependence to account for changes in the effective hard sphere size of realistic solvents whose interactions are actually softer. A reasonable choice to describe the state dependence of σ_{ss} is to equate the isothermal compressibility of the hard sphere fluid determined from CSPT to

Table 1
Least square fit parameters of Eq. (5) to the solvent van der Waals diameters, σ_{ss}, obtained from matching the experimental isothermal compressibilities of water and decane at 20 atm over the entire liquid stable range. Experimental data was taken from the NIST Chemistry Webbook [35]. The diameter and temperature are measure in units of Å and°C respectively.

Parameter	Water	Decane
a_0 (Å)	2.7031	6.8580
a_1 (Å/°C)	1.0262×10^{-3}	-1.4248×10^{-3}
a_2 (Å/°C^2)	-2.3870×10^{-5}	-3.0390×10^{-6}
a_3 (Å/°C^3)	1.4674×10^{-7}	-1.7148×10^{-8}
a_4 (Å/°C^4)	-5.2768×10^{-10}	7.5895×10^{-11}
a_5 (Å/°C^5)	5.9282×10^{13}	-4.5621×10^{13}

the actual compressibility (κ) of the solvent [33]

$$\kappa = \frac{1}{k_B T \rho} \frac{(1-\eta)^4}{(1+2\eta)^2}. \tag{4}$$

The solvent diameter is subsequently adjusted at each state point until the equality holds. This criteria is analogous to the compressibility matching utilized in Weeks, Chandler, Anderson (WCA) perturbation theory that minimizes the free energy difference between a repulsive WCA fluid and hard sphere reference fluid [34]. Fortuitously, Eq. (4) yields physically reasonable solvent diameters even when applied to molecular solvents. Here we fit σ_{ss} values determined from Eq. (4) to a fifth order polynomial of the temperature at fixed pressure

$$\sigma_{ss}(T) = \sum_{i=0}^{5} a_i T^i. \tag{5}$$

A least squares fit of the a_i coefficients to the compressibilities of water and decane are reported in Table 1. The equation-of-state properties of these solvents were taken from the NIST Chemistry Webbook [35]. We use σ_{ss} values of 2.70 Å and 6.77 Å for water and decane, respectively, when we assume the solvent diameter is constant. These diameters where obtained by averaging Eq. (5) over the temperature range 0°C to 100°C. We note that many philosophies have been advocated for determining the effective hard sphere radii of solvents and their temperature dependence, including: fitting to the solubility of noble gases in water in the limit of zero solute polarizability [24]; fitting to the solvent's heat of vaporization [22]; fitting to X-ray scattering experiments [36]; and fitting to the equation-of-state properties of the solvent [37]. Here, we have utilized one of the most frequently used approaches to model solvation properties using CSPT. The equations derived below, however, are applicable to alternate solvent size fitting strategies within the context of CSPT. Moreover, we expect the conclusions drawn here apply in those cases as well, although the specific convergence temperatures may vary in detail.

In Fig. 1 we plot the excess chemical potentials of cavity solutes in water with σ_{cc} = 4 Å, 8 Å, 12 Å, 16 Å and 20 Å from 0°C to 200°C as predicted by CSPT assuming constant (Fig. 1a) and temperature dependent (Fig. 1b) values for σ_{ss}. These calculations were performed at 20 atm to expand the temperature window over which the liquid is stable. Even though the pressure is elevated, these predictions are in near quantitative agreement with those at 1 atm given the pressure differential is not large on a thermodynamic scale. Qualitatively, the curves in both figures agree with one another. The chemical potentials are positive, indicating cavity hydration is generally unfavorable. The chemical potential also grows with solute size, indicating, unsurprisingly, that larger cavities have lower solubilities. The dependence of the cavity chemical potential in both figures is non-monotonic, with a free energy

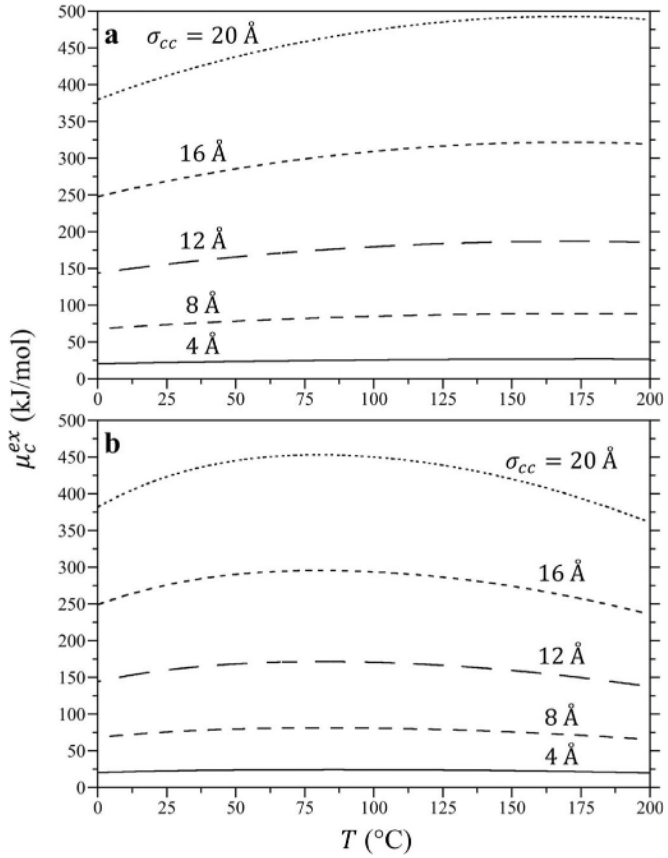

Fig. 1. Excess chemical potentials of hard sphere cavity solutes in water at 20 atm as a function of temperature as predicted by CSPT (Eq. (2)). The solute cavity van der Waals diameters, σ_{cc}, considered were 4 Å, 8 Å, 12 Å, 16 Å, and 20 Å. The curves for each solute are identified in the figure. The two figures indicate predictions assuming a constant value of σ_{ss} = 2.70 Å (a) and a temperature dependent σ_{ss} as described by Eq. (5) (b).

maximum at temperatures above room temperature. This maximum is indicative of the cavity entropy being negative and opposing hydration at room temperature, while changing sign to positive favorable hydration values at elevated temperature. In addition, the significant temperature dependence of the entropy indicates a large positive heat capacity increment of cavity hydration. Taken together, these observations are consistent with CSPT exhibiting the finger prints of hydrophobic hydration discussed above. The main difference between Figs. 1a and b is that the chemical potential maxima, where the hydration entropies are zero, occur at lower temperatures when we assume σ_{ss} is temperature dependent than when it is assumed constant (~80° versus ~170°C). The temperatures bracket the range of experimental convergence temperatures noted above.

The excess hydration entropies of these cavity solutes are plotted in Fig. 2. As anticipated, the hydration entropies of these solutes are strongly temperature dependent, changing sign from negative to positive values with increasing temperature. More importantly, the hydration entropies for these solutes appear to cross one another and converge above room temperature. The convergence occurs near 170°C when we assume a constant σ_{ss} (Fig. 2a), and near 80°C when σ_{ss} varies with temperature (Fig. 2b). These convergence temperatures appear to occur near a hydration entropy of zero, potentially linking the chemical potential maxima and entropy convergence phenomena. Closer examination of the convergence region (*e.g.*, Fig. 2b inset) finds that convergence occurs at negative entropies, as observed experimentally. More inter-

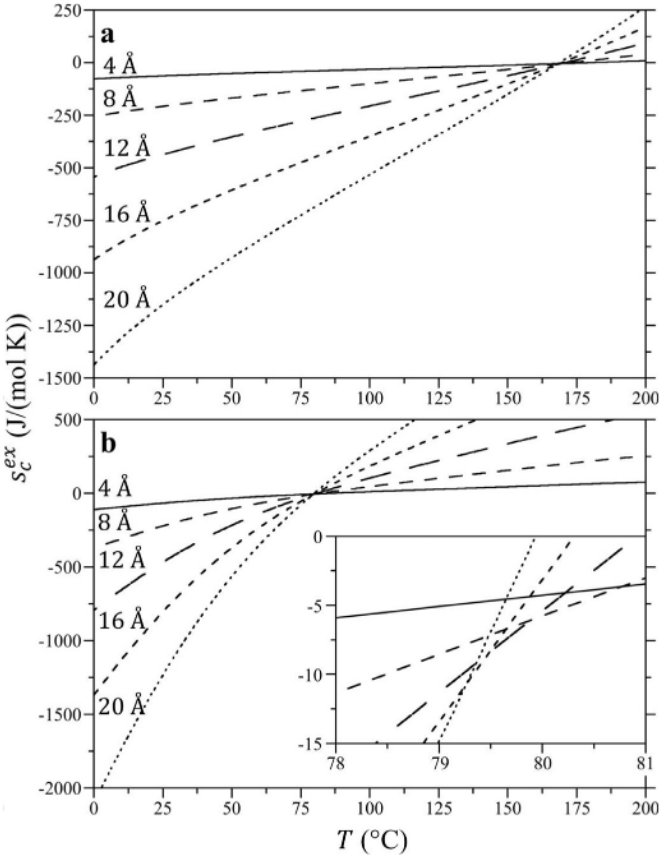

Fig. 2. Excess entropies for hard sphere cavity solutes in water at 20 atm as a function of temperature as predicted by CSPT (Eq. (3)). The solute cavity van der Waals diameters, σ_{cc}, considered were 4 Å, 8 Å, 12 Å, 16 Å, and 20 Å. The curves for each solute are identified in the figure. The two figures indicate predictions assuming a constant σ_{ss} of 2.70 Å (a) and a temperature dependent σ_{ss} as described by Eq. (5) (b). The inset to figure b highlights detail of the entropy convergence region near 80°C.

estingly, the convergence temperature does not appear to be a single temperature, but a narrow range of temperatures over which the entropies of different sized cavities cross one another.

So, what is the origin of the convergence phenomena observed in Fig. 2? To address this question, we consider when does the entropy of a solute of diameter σ_{cc} equal that of one differentially larger by $d\sigma_{cc}$, *i.e.*, when does $s_c^{ex}(\sigma_{cc}) = s_c^{ex}(\sigma_{cc} + d\sigma_{cc})$. This condition is satisfied when the derivative of the entropy with respect to the solute diameter is equal to zero

$$\left.\frac{\partial s_c^{ex}}{\partial \sigma_{cc}}\right|_{P,T} = 0. \tag{6}$$

Taking the solute size derivative of Eq. (3) we can solve for the solute diameter at which the entropy converges (σ_{cc}^*) at a given thermodynamic state point as

$$\sigma_{cc}^* = -\frac{\sigma_{ss}}{2}\frac{\left[\frac{3\eta}{(1-\eta)^2}T\tilde{\alpha} + \frac{3\eta}{(1-\eta)}\left(T\left.\frac{\partial ln\sigma_{ss}}{\partial T}\right|_P - 1\right)\right]}{\left[\frac{3\eta(1+2\eta)}{(1-\eta)^3}T\tilde{\alpha} + \frac{3\eta(2+\eta)}{2(1-\eta)^2}\left(2T\left.\frac{\partial ln\sigma_{ss}}{\partial T}\right|_P - 1\right)\right]}. \tag{7}$$

While this expression can yield negative diameters, corresponding to sub-point like particles in SPT, these are not physically meaningful and outside the range of solute sizes for which Eq. (2) applies. Nevertheless, Eq. (7) also predicts positive diameters at which the entropy converges. Fig. 3 displays the predicted convergence diameters in water assuming σ_{ss} is either constant or temperature dependent. In both cases, the convergence diameter is finite at

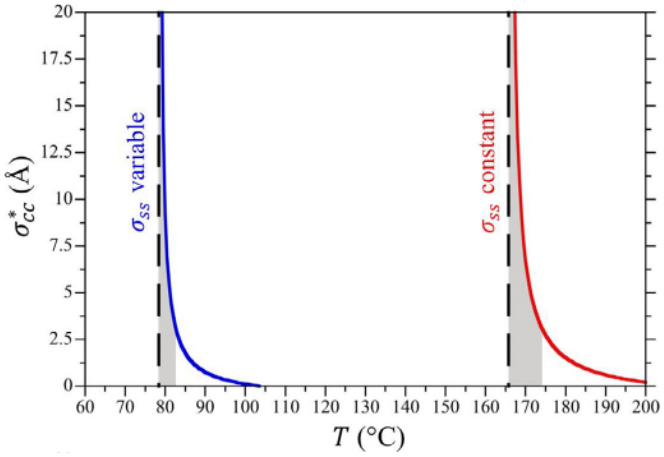

Fig. 3. Solute convergence diameters as a function of temperature at 20 atm as predicted by Eq. (7) in water. The red curve on the right-hand side of the plot indicates predictions assuming a constant σ_{ss} of 2.70 Å, while the blue curve on the left hand side of the plot indicates predictions assuming a temperature dependent σ_{ss} described by Eq. (5). The vertical dashed lines indicate the temperature at which σ_{cc}^* diverges to infinity. The gray shaded regions indicate the range of temperatures entropy convergence is expected to occur for solute cavities 3 Å in diameter and larger.

elevated temperatures and sharply diverges with decreasing temperature. The divergence occurs at 165.7°C for constant σ_{ss} and 78.4°C when it depends on temperature. If we consider the range over which convergence occurs for solute diameters $\sigma_{cc}^* \geq 3$ Å (gray shaded areas in Fig. 3), we find convergence occurs from 165.7°C to 174.3°C (a range of 8.6°C) when σ_{ss} is constant, and 78.4°C to 82.8°C (a range of 4.4°C) when it is temperature dependent. Thus, entropy convergence within CSPT occurs over a narrow range of temperatures for cavities the size of a noble gas atom and larger, giving the appearance of convergence at a single temperature when extrapolated from lower temperatures.

The divergence temperature is determined by the point at which the denominator of Eq. (7) is equal to zero. We then ask, what is the meaning of the divergence temperature? The denominator in Eq. (7) comes from the second order term in σ_{cc} of Eq. (3), *i.e.*, the final term proportional to σ_{cc}^2, which arises from the temperature derivative of the second order term in Eq. (2). This term represents the work associated with expanding the solute's van der Waals area as the solute is grown into solution. As such we expect this term to be related to the surface tension acting on the solute surface. From CSPT, the surface tension for creating a hard, flat interface in solution is

$$\gamma_\infty = \frac{k_B T}{\pi\sigma_{ss}^2}\left[\frac{3\eta(2+\eta)}{2(1-\eta)^2}\right] - \frac{P\sigma_{ss}}{2}. \tag{8}$$

This expression can be derived by dividing the second order term in R of Eq. (1) by $4\pi R^2$, the surface area upon which the compressive solvent force acts on the hard solute. The temperature derivative of the surface tension at constant pressure is

$$\left.\frac{\partial \gamma_\infty}{\partial T}\right|_P = \frac{k_B}{\pi\sigma_{ss}^2}\left[\frac{3\eta(1+2\eta)}{(1-\eta)^3}T\tilde{\alpha} + \frac{3\eta(2+\eta)}{2(1-\eta)^2}\left(2T\left.\frac{\partial ln\sigma_{ss}}{\partial T}\right|_P - 1\right)\right] + \frac{P\sigma_{ss}}{2}\left.\frac{\partial ln\sigma_{ss}}{\partial T}\right|_P \tag{9}$$

Examining Eq. (7), we find that the denominator is proportional to Eq. (9) absent the final term outside the square brackets that is proportional to P. Thus, the divergence in σ_{cc}^* predicted by Eq. (7) is determined by the temperature at which the derivative of the surface tension predicted by CSPT less the pressure contribution ($P\sigma_{ss}/2$) is zero. At atmospheric pressure, the pressure con-

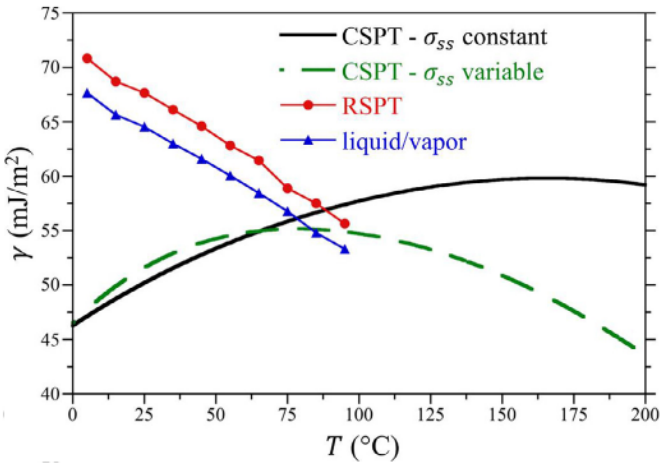

Fig. 4. Surface tension of water predicted from scaled particle theory and molecular simulation as a function of temperature. CSPT predictions for the surface tension of water against a hard surface (Eq. (8)) are reported assuming a constant σ_{ss} of 2.70 Å and a temperature dependent σ_{ss} described by Eq. (5). RSPT fits to simulations of cavities in water and the surface tension of the water liquid/vapor interface determined from simulation are also reported. The figure symbols are defined in the legend. The simulation results were previously reported in ref. [30]. The water model used in those simulations was TIP4P/2005 [38].

tribution to Eq. (8) is ~0.01 mJ/m^2 (0.02%) of the overall surface tension and can subsequently be neglected. It may be concluded that the entropy convergence in Fig. 2 is dictated by the temperature dependence of the surface tension predicted by CSPT at ambient conditions. The observed convergence then is simply a result of the surface area contribution to the entropy in Eq. (3) that dominates as the solute size increases.

A consequence of the temperature derivative of the surface tension being zero is that the surface tension must exhibit an extremum at that point. In Fig. 4 we plot the temperature dependence of the surface tension as predicted by Eq. (8). As anticipated, we find maxima in γ_∞ coincident with the divergences reported in Fig. 3 using a constant and temperature dependent σ_{ss}. At low pressures it is thought that the surface tension predicted by SPT is closely related to the surface tension associated with creating a liquid/vapor interface. The reason for this presumption at low pressure is that the solvent density in contact with a flat, hard interface is akin to that of a vapor, which transitions to the liquid density at more distant separations through a liquid/vapor interface [29]. The proximity of the hard surface, however, could certainly perturb the surface tension, although the effect is thought to be small. Given that liquid/vapor surface tensions are generally decreasing functions of temperature it is somewhat surprising that CSPT predicts a maximum in the interfacial tension of water! A decrease in the interfacial tension reflects a positive entropy of interface formation. Given that water must forfeit hydrogen bonds to approach a flat interface and the vapor film adjacent to the surface imparts more freedom to the waters in that layer, it is difficult to rationalize a negative surface entropy that raises the surface tension with increasing temperature. We ask then, is the non-monotonic dependence of the surface tension predicted by SPT reasonable? Previously, we reported molecular simulations of repulsive spherical solutes of varying size in TIP4P/2005 water [38] over a range of temperatures and pressures [30]. By considering the solvent forces acting on the solute surface, we determined the surface tension of water against a hard interface using RSPT. In Fig. 4 we compare the surface tensions obtained from RSPT and the liquid/vapor surface tensions of TIP4P/2005 water against the predictions of CSPT. In difference to CSPT, RSPT obtains a surface tension that is a decreasing function of temperature that is parallel to the surface tension of the liquid/vapor interface. The RSPT surface tension is only ~5% greater than that of the liquid/vapor interface over the simulated temperature range. Similar differences between RSPT and liquid/vapor surface tension have also been observed for solvation in the Lennard-Jones [31,39] and Jagla [40] liquids. This surface tension difference has been attributed to the suppression of capillary fluctuations against the hard surface relative to the liquid/vapor interface. It may be concluded that the non-monotonic dependence of water's surface tension predicted by CSPT results from the neglect of inter-molecular correlations to arrive at an analytical expression for the free energy. It follows that the entropy convergence predicted by CSPT is an artifact of the incorrect temperature dependence of the surface tension predicted by the theory.

CSPT has enjoyed success, however, in capturing the curious non-monotonic temperature dependence of the free energy of hydrophobic hydration that underlies many of its thermodynamic puzzles. We ask then, are CSPT predictions unique for water as a solvent? It is reasonable to associate the maxima in the chemical potentials reported in Fig. 1 with the divergences reported in Fig. 3 given that entropy convergence occurs near the temperature the entropy is zero. This is equivalent to assuming the entropy is dominated by the surface area dependent contribution in Eq. (3) for sufficiently large solutes. Setting the denominator of Eq. (7) equal to zero we arrive at the estimate

$$T\tilde{\alpha} = \frac{(2+\eta)(1-\eta)}{2(1+2\eta)}\left(1 - 2T\left.\frac{\partial ln\sigma_{ss}}{\partial T}\right|_P\right) \tag{10}$$

for the temperature the excess chemical potential is at an extremum and entropy convergence occurs for large solutes. When $T\tilde{\alpha}$ is less than the right-hand side of this expression the surface tension is an increasing function of the temperature, while when it is greater than the right-hand side the surface tension is a decreasing function of the temperature. Assuming σ_{ss} is constant, $\tilde{\alpha}$ reduces to the thermal expansion coefficient. It is well known that the thermal expansivity of water is a significantly increasing function of temperature that initially starts off below zero at 0°C and changes sign at the temperature of maximum density (4°C). Since the right-hand side Eq. (10) is positive when σ_{ss} is fixed, we expect the chemical potential to be an initially increasing function of temperature with an associated negative entropy. As the thermal expansivity increases at a high enough temperature Eq. (10) is eventually satisfied and the chemical potential shortly thereafter decreases with increasing temperature. Thus, it may be concluded that the maxima in the chemical potential of hydrophobic hydration results from the distinctive equation-of-state properties of liquid water as manifest in the temperature dependence of its thermal expansivity. If we relax the assumption that σ_{ss} is constant, we find that the chemical potential maximum shifts to lower temperatures as a result of σ_{ss} largely being a decreasing function of temperature.

Despite the assertion that the maxima in the chemical potential of non-polar cavity hydration results from the unique temperature dependence of water's thermal expansivity, we test this conclusion by examining the predictions of CSPT for a model organic solvent. In Fig. 5 we report the chemical potentials of cavity solvation in decane as a function of temperature at 20 atm for cavity diameters of 4 Å, 8 Å, 12 Å, 16 Å, and 20 Å as predicted by Eq. (2). These free energies are generally lower than those in water by half, keeping with the observation that cavities are more insoluble in smaller diameter solvents as a result of the lower available free volume to accommodate the solute. Notably, we find that CSPT predicts a weak maximum in the chemical potential near 40°C when we assume σ_{ss} is constant (Fig. 5a), indicative of the entropy changing sign from negative to positive with increasing temperature. On the other hand, the cavity solvation free energy is found to be a decreasing function of temperature when σ_{ss} is temperature depen-

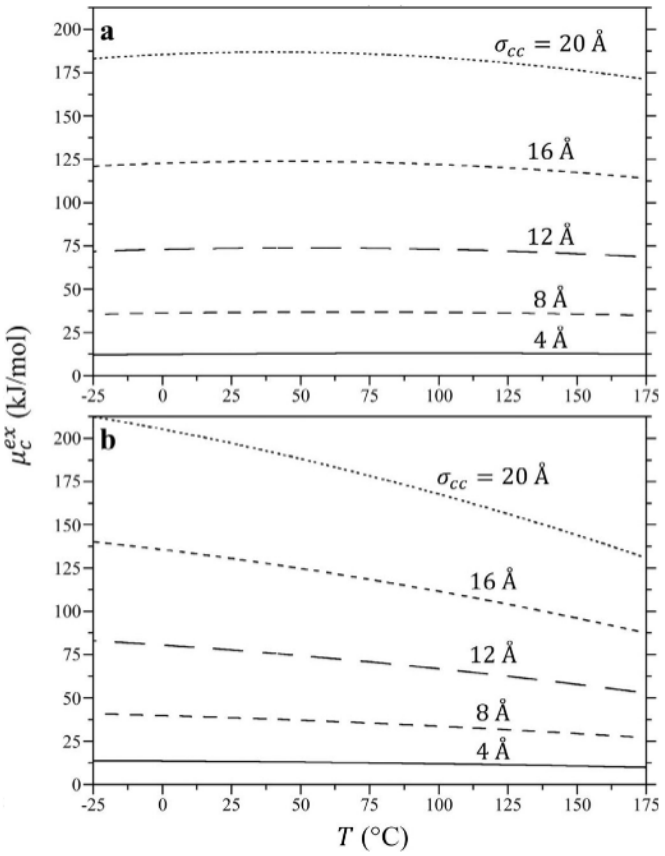

Fig. 5. Excess chemical potentials of hard sphere cavity solutes in decane at 20 atm as a function of temperature as predicted by CSPT (Eq. (2)). The solute cavity van der Waals diameters, σ_{cc}, considered were 4 Å, 8 Å, 12 Å, 16 Å, and 20 Å. The curves for each solute are identified in the figure. The two figures indicate predictions assuming a constant value of σ_{ss} = 6.77 Å (a) and a temperature dependent σ_{ss} as described by Eq. (5) (b).

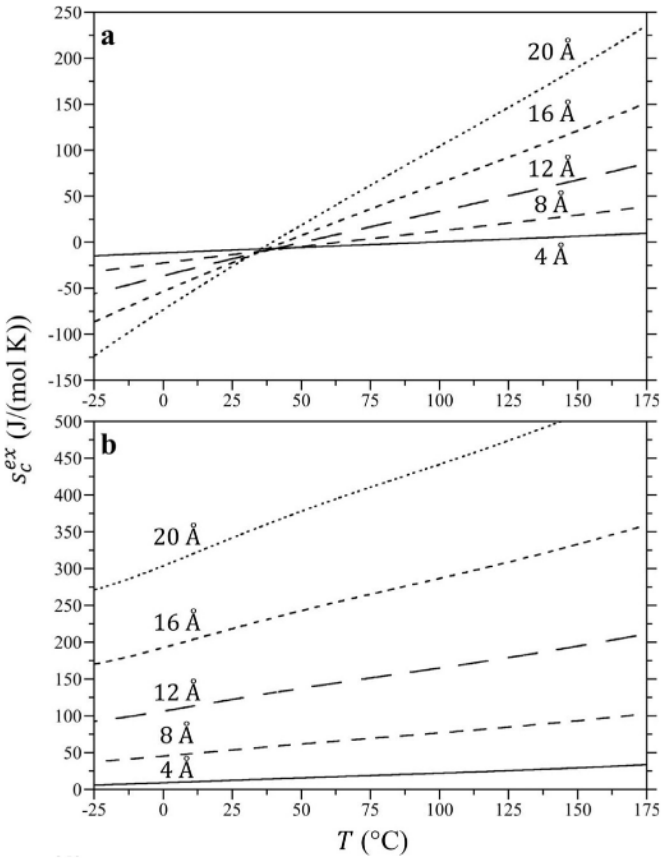

Fig. 6. Excess entropies for hard sphere cavity solutes in decane at 20 atm as a function of temperature as predicted by CSPT (Eq. (3)). The solute cavity van der Waals diameters, σ_{cc}, considered were 4 Å, 8 Å, 12 Å, 16 Å, and 20 Å. The curves for each solute are identified in the figure. The two figures indicate predictions assuming a constant value of σ_{ss} = 6.77 Å (a) and a temperature dependent σ_{ss} as described by Eq. (5) (b).

dent (Fig. 5b). When we consider the solvation entropies in decane we observe apparent convergence near 40°C for constant σ_{ss} (Fig. 6a), while no entropy crossing is found when σ_{ss} depends on temperature (Fig. 6b). These observations conflict with the conclusion that entropy convergence results from the unique equation-of-state properties of water, although we note that convergence can disappear when σ_{ss} depends on temperature.

In Fig. 7 we report the convergence diameters for cavity solvation in decane obtained from Eq. (7). Assuming a constant σ_{ss}, σ_{cc}^* diverges at 22.4°C, somewhat lower than the temperature at which the solvation entropies appear to cross one another in Fig. 6a. If we consider the convergence temperatures for cavities with $\sigma_{cc}^* \geq$ 3 Å (shaded in gray in Fig. 7), we find they span from 22.4°C to 85.8°C (a range of 63.4°C). So, while the solvation entropies cross one another in decane when σ_{ss} is constant, the range of crossing points is an order of magnitude broader than in water. While entropy convergence is not observed when σ_{ss} is temperature dependent for cavity diameters 4 Å and larger (Fig. 6), Eq. (7) predicts sub-atomic crossing diameters 1 Å and smaller at the lowest temperatures considered (Fig. 7). It may be surmised then the crossing diameter will diverge with decreasing temperature, although this occurs well below decane's freezing point.

As discussed above, the divergence in σ_{cc}^* implies the surface tension predicted by CSPT exhibits a maximum near that temperature. Assuming σ_{ss} is constant, CSPT does indeed predict a non-monotonic temperature dependence of the surface tension (Fig. 8). The surface tension becomes a monotonically decreasing function of temperature, however, when σ_{ss} is temperature de-

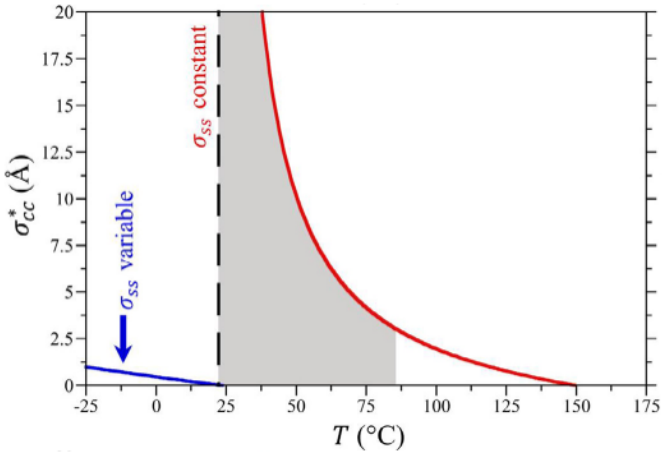

Fig. 7. Solute convergence diameters as a function of temperature at 20 atm as predicted by Eq. (7) in decane. The red curve on the right-hand side of the plot indicates predictions assuming a constant σ_{ss} of 6.77 Å, while the blue curve on the left-hand side of the plot indicates the predictions assuming a temperature dependent σ_{ss} described by Eq. (5). The vertical dashed lines indicate the temperature at which σ_{cc}^* diverges to infinity. The gray shaded region indicates the range of temperatures entropy convergence is expected to occur for solute cavities 3 Å in diameter and larger.

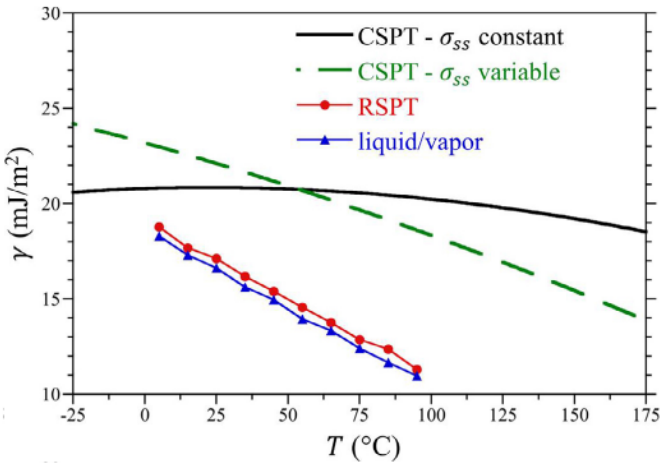

Fig. 8. Surface tension of decane predicted from scaled particle theory and molecular simulation as a function of temperature. CSPT predictions for the surface tension of decane against a hard surface (Eq. (8)) are reported assuming a constant σ_{ss} of 6.77 Å and a temperature dependent σ_{ss} described by Eq. (5). RSPT fits to simulations of cavities in decane and the surface tension of the decane liquid/vapor interface determined from simulation are also reported. The figure symbols are defined in the legend. The simulation results were previously reported in ref. [30]. The decane model used in those simulations was TraPPE-UA [41].

pendent (Fig. 8). The surface tensions of decane determined from molecular simulation using RSPT and from the liquid/vapor interface closely track one another (Fig. 8) [30]. The surface tension of decane against the hard surface determined from simulations of TraPPE/UA decane [41] using RSPT [30] is found to be ~3% larger than that obtained from the liquid/vapor interface, similar to the differences observed in water (Fig. 4). These simulation surface tensions are decreasing functions of temperature, as expected for the formation of a liquid/vapor interface. This comparison further highlights the unphysical CSPT prediction that the surface tension against a hard surface can vary non-monotonically with temperature, which resultantly impacts the veracity of the CSPT prediction that solvation entropies converge at a distinct temperature.

While we have not considered the impact of the cavity shape on entropy convergence here, morphometric thermodynamics [42] predicts that the leading order terms in the excess chemical potential of hard, convex solutes are

$$\mu_c^{ex} = PV + \gamma_\infty A + lower\ order\ terms, \quad (11)$$

where V and A are the cavity's solvent accessible volume and area, respectively. So, while CSPT predicts an entropy convergence temperature for prolate and oblate spherocylinders in water that agree with that of spheres [28], this prediction should not be surprising given the dominance of the predicted non-monotonic dependence of γ_∞ on temperature. When a more realistic temperature dependence of γ_∞ is incorporated into the theory, the entropy convergence is expected to be smeared out over a wide temperature range depending on the solute size [10].

In summary, we have examined the origin of solvation entropy convergence phenomena as predicted by classic scaled particle theory. We demonstrated that if the surface tension against a hard surface is predicted to vary non-monotonically with temperature, the cavity solvation entropy exhibits entropy convergence. The temperature dependence predicted by CSPT, however, is unphysical. Using a revised version of SPT that incorporates molecular details and multi-body correlations beyond the effective solvent diameter and density, the non-monotonic temperature dependence of the surface tension disappears and washes away the observation of a distinct convergence temperature [10]. While the prediction of entropy convergence by CSPT has been ascribed to the unique equation-of-state properties of liquid water, and by association its hydrogen bonding properties, we demonstrated CSPT can also predict entropy convergence in decane. The occurrence of entropy convergence in decane can be mitigated by utilizing a temperature dependent solvent diameter, although this temperature dependence is empirical and obscures the molecular interpretation of solvation phenomena. While higher order curvature corrections can contribute to the range of temperatures over which convergence is observed (*e.g.*, Figs. 3 and 7), the convergence temperature with increasing solute size it drawn to the convergence criteria established by Eq. (10) as a result of the dominance of surface contributions with increasing solute size.

We may naturally ask, why do experimental hydration entropies of a number of classes of solutes appear to converge? While beyond the scope of this work, convergence has been observed from simulations over a limited range of solute sizes [16]. Moreover, we have demonstrated for *n*-alkanes that the packing and correlations of water with the solute are determined largely by the local molecular details rather than an effective spherical diameter for the solute [43]. Given that the hydration entropy can be expanded in terms of local correlations of alkanes with water, entropy convergence for a given family of solutes is perhaps not unexpected. Indeed, hydration entropies scaled by the surface areas of a large number of alkanes and aromatic hydrocarbons have been shown from simulation to collapse onto two distinct curves depending on the degree of bond saturation [44]. This is bolstered by the fact that group additivity approximations have proven useful in correlating hydration thermodynamic results [9,45,46].

Declaration of Competing Interest

The authors declare that they have no known competing financial interests or personal relationships that could have appeared to influence the work reported in this paper.

Acknowledgements

We gratefully acknowledge financial support from the National Science Foundation (CBET-1805167). In addition, we thank Nuno Galamba (Lisbon) for helpful conversations.

Author Statement

Henry S. Ashbaugh performed all the analyses contained herein and wrote this manuscript.

References

[1] C. Tanford, The Hydrophobic Effect: Formation of Micelles and Biologi-cal Membranes, Wiley, New York, 1980.
[2] W. Blokzijl, J. Engberts, Hydrophobic effects – Opinions and facts, Angew. Chem.-Int. Edit 32 (1993) 1545–1579.
[3] H.S. Frank, M.W. Evans, Free volume and entropy in condensed systems III. Entropy in binary liquid mixtures; partial molal entropy in dilute solutions; structure and thermodynamics in aqueous electrolytes, J. Chem. Phys. 13 (1945) 507–532.
[4] J.A.V. Butler, W.S. Reid, The solubility of non-electrolytes. Part III. The entropy of hydration, Journal of the Chemical Society (1936) 1171–1173.
[5] H.S. Ashbaugh, H. Bukannan, pressure Temperature, Temperature, pressure, and concentration derivatives of nonpolar gas hydration: Impact on the heat capacity, temperature of maximum density, and speed of sound of aqueous mixtures, J. Phys. Chem. B 124 (2020) 6924–6942.
[6] K.P. Murphy, P.L. Privalov, S.J. Gill, Common Features of Protein Unfolding and Dissolution of Hydrophobic Compounds, Science 247 (1990) 559–561.
[7] B. Lee, Isoenthalpic and isoentropic temperatures and the thermodynamics of proteindenaturation, Proc. Natl. Acad. Sci. USA 88 (1991) 5154–5185.
[8] L. Fu, E. Freire, On the origin of the enthalpy and entropy convergence temperatures in protein folding, Proc. Natl. Acad. Sci. USA 89 (1992) 9335–9338.
[9] P.L. Privalov, G.I. Makhatadze, Contribution of hydration to protein folding thermodynamics, J. Mol. Biol. 232 (1993) 660–679.
[10] H.S. Ashbaugh, L.R. Pratt, Colloquium: Scaled particle theory and the length scales of hydrophobicity, Rev. Mod. Phys. 78 (2006) 159–178.

[11] R.L. Baldwin, Temperature dependence of the hydrophobic interaction in protein folding, Proc. Natl. Acad. Sci. USA 83 (1986) 8069–8072.
[12] G. Graziano, Entropy convergence in the hydration thermodynamics of n-alcohols, J. Phys. Chem. B 109 (2005) 12160–12166.
[13] R.L. Baldwin, N. Muller, Relation bether the convergence temperatures Th and Ts in protein unfolding, Proc. Natl. Acad. Sci. USA 89 (1992) 7110–7113.
[14] W. Kauzmann, Some factors in the interpretationof protein denaturation, Adv. Protein Chem. 14 (1959) 1–63.
[15] A.D. Robertson, K.P. Murphy, Protein structure and the energetics of protein stability, Chem. Rev. 97 (1997) 1251–1267.
[16] S. Garde, G. Hummer, A.E. Garcia, M.E. Paulaitis, L.R. Pratt, Origin of entropy convergence in hydrophobic hydration and protein folding, Phys. Rev. Lett. 77 (1996) 4966–4968.
[17] F. Sedlmeier, D. Horinek, R.R. Netz, Entropy and enthalpy convergence of hydrophobic solvation beyond the hard-sphere limit, J. Chem. Phys. 134 (2011) 055105.
[18] F. Sedlmeier, R.R. Netz, The spontaneous curvature of the water-hydrophobe interface, J. Chem. Phys. 137 (2012) 14.
[19] D.M. Huang, D. Chandler, Temperature and length scale dependence of hydrophobic effects and their possible implications for protein folding, Proc. Natl. Acad. Sci. U. S. A. 97 (2000) 8324–8327.
[20] K. Lum, D. Chandler, J.D. Weeks, Hydrophobicity at small and large length scales, J. Phys. Chem. B 103 (1999) 4570–4577.
[21] H. Reiss, H.L. Frisch, J.L. Lebowitz, Statistical mechanics of rigid spheres, J. Chem. Phys. 31 (1959) 369–380.
[22] H. Reiss, H.L. Frisch, E. Helfand, J.L. Lebowitz, Aspects of the StatisticalThermodynamics of Real Fluids, J. Chem. Phys. 32 (1960) 119–124.
[23] H. Reiss, Adv. Chem. Phys 9 (1965) 1.
[24] R.A. Pierotti, Aqueous solutions of nonpolar gases, J. Phys. Chem. 69 (1965) 281–288.
[25] R.A. Pierotti, Scaled-particle theory of dilute aqueous solutions, J. Phys. Chem. 71 (1967) 2366–2367.
[26] R.A. Pierotti, A scaled particle theory of aqueous and nonaqueous solutions, Chem. Rev. 76 (1976) 717–726.
[27] G. Graziano, B. Lee, Entropy convergence in hydrophobic hydration: a scaled particle theory analysis, Biophys. Chem. 105 (2003) 241–250.
[28] A. Grimaldi, G. Graziano, A reassessment of entropy convergence in solvation thermodynamics, J. Mol. Liq. 269 (2018) 119–125.
[29] F.H. Stillinger, J. Soultion Chem 2 (1973) 141.
[30] H.S. Ashbaugh, N.D. Moura, H. Houser, Y. Wang, A. Goodson, J.W. Barnett, Temperature and pressure dependence of the interfacial free energy against a hard surface in contact with water and decane, J. Chem. Phys. 145 (2016) 10.
[31] H.S. Ashbaugh, Blowing bubbles in Lennard-Jonesium along the saturation curve, J. Chem. Phys. 130 (2009) 8.
[32] A. Bennaim, Standard thermodynamics of transfer - Uses and misuses, J. Phys. Chem. 82 (1978) 792–803.
[33] S.W. Mayer, Dependence of surface tension on temperature, J. Chem. Phys. 38 (1963) 1803–1808.
[34] J.D. Weeks, D. Chandler, H.C. Andersen, Role of repulsive forces in determin the equilibrium structure of simple liquids, J. Chem. Phys. 54 (1971) 5237–5247.
[35] NIST Standard Reference Database Number 69. https://webbook.nist.gov/chemistry/.
[36] A. Bondi, van der Waals volumes and radii, J. Phys. Chem 68 (1964) 441–451.
[37] B.-A.-. D., D.R. Herschback, Estimation of the effective diameter for molecular fluids, J. Phys. Chem. B 95 (1990) 1038–1047.
[38] J.L.F. Abascal, C. Vega, A general purpose model for the condensed phases of water: TIP4P/2005, J. Chem. Phys. 123 (2005) 12.
[39] M.P. Moody, P. Attard, Curvature dependent surface tension from a simulation of a cavity in a Lennard-Jones liquid close to coexistence, J. Chem. Phys. 115 (2001) 8967–8977.
[40] J.R. Dowdle, S.V. Buldyrev, H.E. Stanley, P.G. Debenedetti, P.J. Rossky, Temperature and length scale dependence of solvophobic solvation in a single-site water-like liquid, J. Chem. Phys. 138 (2013) 12.
[41] M.G. Martin, J.I. Siepmann, Transferable potentials for phase equilibria. 1. United-atom description of n-alkanes, J. Phys. Chem. B 102 (1998) 2569–2577.
[42] Z.H. Jin, J. Kim, J.Z. Wu, Shape Effect on Nanoparticle Solvation: A Comparison of Morphometric Thermodynamics and Microscopic Theories, Langmuir 28 (2012) 6997–7006.
[43] H.S. Ashbaugh, M.E. Paulaitis, Entropy of hydrophobic hydration: Extension to hydrophobic chains, J. Phys. Chem. 100 (1996) 1900–1913.
[44] K. Tamoliūnas, N. Galambaa, Protein Denaturation, Zero Entropy Convergence, and the Structure of Water around Hydrophobic and Amphiphilic Solutes. submitted.
[45] N.V. Plyasunova, A.V. Plyasunov, E.L. Shock, Database of thermodynamic properties for aqueous organic compounds, Intern. J. Thermophys. 25 (2004) 351–360.
[46] T. Ooi, M. Oobatake, G. Nemethy, H.A. Scheraga, Accessible surface areas as a measure of the thermodynamic parameters of hydration of peptides, Proc. Natl. Acad. Sci. USA 84 (1987) 3086–3090.